 doi:10.20944/preprints202103.0411.v1

Article

AAV-HDV an attractive platform for the in vivo study of HDV biology and mechanism of disease pathogenesis

Sheila Maestro[1,2], Nahia Gomez-Echarte[1,2], Gracian Camps[1,2], Carla Usai[1,2#], Lester Suarez[3], Africa Vales[1,2], Cristina Olagüe[1,2], Rafael Aldabe[1,2*] and Gloria González- Aseguinolaza[1,2*].

[1] Universidad de Navarra, CIMA, Programa de Terapia Génica y Regulación de la Expresión Génica, Avenida Pío XII, 31080, Pamplona, España.
[2] IdiSNA, Instituto de Investigación Sanitaria de Navarra.
[3] AskBio. 20 TW Alexander Drive , Suite 110 Research Triangle Park, NC 27709
#Current address: Blizard Institute, Centre for Immunobiology 4 Newark St London United Kingdom E1 2AT

* Correspondence: raldabe@unav.es; ggasegui@unav.es; Tel.: +34 948194700x4024 (RA); +34 948194700x4024 (GGA).

In memoriam: Dr. Ricardo Flores

Abstract:

Hepatitis delta virus (HDV) infection causes the most severe form of viral hepatitis but little is known about the molecular mechanisms involved. The recently developed HDV mouse model based on the delivery of HDV replication-competent genomes using adeno-associated vectors (AAV) develop a liver pathology very similar to the human disease, and allowed us to perform mechanistic studies. We have generated different AAV-HDV mutants to eliminate the expression HDV antigens (HDAgs), characterized them both *in vitro* and *in vivo*. We confirmed that S-HDAg is essential for HDV replication and cannot be replaced by L-HDAg or host cellular proteins, and the L-HDAg is essential for HDV infectious particle production. We have also found that the lack of L-HDAg resulted in the increase of of S-HDAg expression levels and the exacerbation of liver damage which is T cell independent but is associated with an increment in liver inflammation. Interestingly, early expression of L-HDAg significantly ameliorated the liver damage induced by the mutant expressing only the S-HDAg. In summary, the use of AAV-HDV represents a very attractive platform to interrogate *in vivo* the role of viral components in the HDV life cycle and to better understand the mechanism of HDV-induced liver pathology.

Keywords: HDV; mouse model; AAV, HDAg, Liver damage.

1. Introduction

Hepatitis delta virus (HDV) is a satellite virus that requires hepadnavirus envelope proteins for its transmission. Approximately 5% of HBV carriers have been exposed to HDV, with a total of 15-20 million patients worldwide, although recent studies reported higher prevalence numbers [1-3]. HDV infection is associated with the most severe form of viral hepatitis with a twofold higher risk of developing cirrhosis, a threefold higher risk of developing hepatocellular carcinoma (HCC), and two fold increased mortality in comparison with HBV monoinfection [4-6]. Despite recent advances in the management of this condition, it still represents a significant medical burden [6-8]. Furthermore, the mechanisms associated with the severity of the disease remains unknown although it is thought to be associated to the host immune response, since a significant inflammatory infiltrate composed of

Preprints (www.preprints.org) | NOT PEER-REVIEWED | Posted: 16 March 2021 doi:10.20944/preprints202103.0411.v1

macrophages and lymphocytes is observed in the liver of HDV patients [9,10]. However, HDV has been also considered to be directly cytopathic particularly during the acute stage of infection and it has been related to the expression of viral antigens [11-13].

HDV is a defective RNA virus that requires the surface antigens of hepatitis B virus (HBV) (HBsAg) for viral assembly and transmission [14]. Specific interaction between HBsAg and the human Na+/taurocholate cotransporting polypeptide (hNTCP) determines the hepatotropism and species-specificity of both viruses [15,16]. Although NTCP is also expressed in mouse livers, mice are resistant to HBV and HDV infections due to small differences between the human and mouse NTCP protein sequences [16].

The HDV genome is a circular negative-sense RNA molecule of approximately 1,700 nucleotides that appears as a double-stranded rod-like structure. It contains a single open reading frame that encodes two HDV antigens (HDAgs), a 24 kDa small HDV antigen (S-HDAg) and a 27 kDa large HDV antigen (L-HDAg) of 195 and 214 amino acids, respectively. Despite sharing most of their amino acid sequence they differ significantly in their functions: it has been described that S-HDAg is essential for HDV replication, whilst L-HDAg blocks HDV replication and is essential for viral assembly [14,17-19]. The production of the L-HDAg required RNA editing at adenosine 1012 (amber/W site) in the antigenomic RNA sequence by host adenosine deaminases that act on RNA (ADARs) [20].

All this studies have been performed in cell culture due to the lack of an *in vivo* model in which the HDV genome can be easily manipulated and tested.

Recently, we developed a mouse model of HDV replication, based on adeno-associated viral vector (AAV)-mediated delivery of HBV and HDV replication-competent genomes to the liver. This model mimics most of the features of HDV infection in humans, including the induction of liver inflammation and liver injury in association with the expression of genes involved in the development of HCC, cirrhosis, fibrosis, and cell death [21]. Using this model, we described that MAVS was responsible for the strong type I IFN response induced by HDV replication observed in cell lulture and in animal models [21-24]. This result was corroborated later on in human hepatic cells identifying MDA5 as the main cellular pattern recognition receptor (PRR) involved in HDV detection that signals through MAVS and induces IFN-β gene transcription [25]. Furthermore, the involvement of TNF-α in the HDV-induced pathology was demonstrated using this animal model and it was confirmed by the amelioration of liver damage in AAV-HBV/HDV injected animals treated with Etanercept, which blocks the TNF-α signaling pathway [26].

One of the beauties of this model is that it allows genetic modification of HDV viral genomes that can be then tested in cell culture and more importantly in the liver of mice to interrogate the role of viral components in the viral life cycle and in the induction of liver pathology. Furthermore, the establishment of HDV replication in genetically manipulated mice allows to analyse the involvement of different host factors.

The aim of this work was to determine the role of HDV antigens in HDV-mediated liver injury using AAV-HDV carrying different mutations.

2. Materials and Methods

Plasmids and AAV vectors

The AAV-HDV wt plasmid was generated as previously described by cloning the HDV 1.2x (genotype 1) genome sequence obtainned from the plasmid pDL456 (kindly provide by J. M. Taylor) under the control of a hepato-specific promoter into the AAV-MCS plasmid [21]. Different HDV mutants were created by introducing point mutations. All the plasmids were generated with the In-Fusion® HD Cloning Kit (Takara Bio USA) following the manufacturer's instructions. To that end, the coding sequence of HDAg was amplified with primers that contain the desired mutation. Firstly, HDV-ΔS-HDAg, HDV-ΔL-HDAg, and HDV-ΔHDAg mutants were produced in order to block the expression of either S-HDAg, L-HDAg, or both, respectively. The first mutant contains a single

Preprints (www.preprints.org) | NOT PEER-REVIEWED | Posted: 16 March 2021 doi:10.20944/preprints202103.0411.v1

nucleotide change (A/G) in the editable amber stop codon 1014-1015 (TAG) which produces a tryptophan codon (TGG) that cannot be edited, leading always to the production of the L-HDAg. The second one contains another point mutation (G/A) that changes the amber stop codon (TAG) for another stop codon (TAA) that cannot be converted into a tryptophan codon by ADAR [20]. Therefore, from this sequence, only the S-HDAg will be produced. For the construction of the HDV-ΔHDAg mutant, the start codons found in the sequence (located between nucleotides 1088-1090 and 1364-1366) were replaced by stop codons (TAA). AAV-HBV plasmid was constructed by insertion of 1.3x copies of the HBV genome (genotype D, serotype ayw) obtained from the pSP65 plasmid (kindly provided by Dr. Francis Chisari) into pAAV-MCS [21].

The recombinant AAV genomes were encapsidated in the mouse liver tropic AAV serotype 8 capsid. Briefly, each AAV vector plasmid and the helper/packaging plasmid pDP8.ape (Plasmid factory, Bielefeld, Germany) were co-transfected into HEK-293T cells. The cells and supernatants were harvested 72 h after transfection and virus was released from the cells by three rounds of freeze-thawing. Crude lysate from all batches was then treated with DNAse and RNAse (0.1mg per p150 culture dish) for 1 hour at 37°C and then kept at −80°C until purification. Purification of crude lysate was performed by ultracentrifugation in Optiprep Density Gradient Medium-Iodixanol (Sigma-Aldrich, St Louis MO). Thereafter, iodioxanol was removed and the batches were concentrated by passage through Amicon Ultra-15 tubes (Ultracel-100K; Merck Millipore, Cork Ireland). For virus titration, viral DNA was isolated using the High Pure Viral Nucleic Acid kit (Roche Applied Science. Mannheim, Germany). Viral titers in terms of genome copies per milliliter (vg/ml) were determined by qPCR (Applied Biosystems, Foster City, CA).

Animals and treatment

C57BL/6 mice were purchased from Harlan Laboratories (Barcelona, Spain). Rag1 (Rag1 KO) on a C57BL/6 genetic background, were bred and maintained at the animal facility of the University of Navarra. Six- to eight-weeks-old male mice were used in all experiments. Mice were kept under controlled temperature, light, and pathogen-free conditions. Mice were injected intravenously (i.v.) with the AAV vectors (5 x 10^{10} viral genomes (vg)/mouse) in a volume of 100 µl. For all procedures, animals were anesthetized by intraperitoneal (i.p.) injection of a mixture of xylazine (Rompun 2%, Bayer) and ketamine (Imalgene 50, Merial) 1:9 v/v or by isoflurane inhalation. Blood collection was performed by submandibular bleeding, and serum samples were obtained after centrifugation of total blood. Animals were euthanized by cervical dislocation after being anesthetized. The experimental design was approved by the Ethics Committee for Animal Testing of the University of Navarra (R-132-19GN).

Cell lines

Two human hepatoma cell lines, HepG2 and Huh7, were transfected with the HDV WT-encoding plasmids, while the characterization of HDV-ΔL-HDAg, HDV-ΔS-HDAg and HDV-ΔHDAg mutants was only performed in Huh-7 cells. Moreover, Huh7-hNTCP cells, kindly provided by Dr. Urtzi Garaigorta, were employed for infectivity studies. HepG2 and Huh-7 cell lines were cultured in Dulbecco's modified Eagle's medium (DMEM) supplemented with 10% fetal bovine serum (FBS), 1% of L-glutamine, 1% of glucose, 100 U/ml of penicillin-streptomycin, and nonessential amino acids, and incubated at 37°C with 5% CO2 in a humidified atmosphere. In the case of Huh7-hNTCP cells, the culture medium was supplemented with 2.5 µg/ml blasticidine to ensure the selection of hNTCP-expressing cells.

DNA transfection

For the comparative study of HDV transfection in HepG2 and Huh7 cells, both cell lines were seeded and transfected in parallel. Briefly, 3.5x10^5 HepG2 and Huh-7 cells were seeded per well in 6-well

 doi:10.20944/preprints202103.0411.v1

plates and maintained in DMEM 10% FBS. After 24h, or when cells reached 80-90% confluence, the medium was substituted by Opti-mem and cells were transfected with 2.5µg DNA/well using Lipofectamine 3000, following the manufacturer's instructions. 4-6 h later, cells were supplemented with 1.5ml of DMEM 10% FBS and the day after, the medium containing the transfection reagents was replaced by fresh DMEM. Cells were then collected at different time points until 14 days post-transfection (dpt). At 7 dpt, cells were trypsinized, split 1:3 and reseed in new wells.

Cell fractionation, protein extraction and quantification

Harvested cells were resuspended in the RIPA lysis buffer supplemented with 1% PMSF (phenylmethylsulfonyl fluoride), 1% protease inhibitor cocktail, and 0.1% of sodium orthovanadate, and incubated on ice for 30 min. Cell extracts were then spun for 20 min at 13000 rpm and 4ºC and supernatants were collected for western blot analysis.

To determine the intracellular location of the proteins cells were harvested with Trypsin-EDTA and centrifuged for 5 min at 500g and 4ºC. Then, proteins of each cellular compartment were separated with the Subcellular Protein Fractionation Kit (Thermo Scientific). To quantify protein concentration, a BCA protein assay kit was used (Thermo Scientific) and a standard curve of increasing concentrations of BSA (Bovine Serum Albumin).

Western blot

Equal amounts of protein were loaded in a SDS-polyacrylamide gel, separated by electrophoresis, and transferred onto a nitrocellulose membrane by electroelution. After a 45 min blockade with TBS-tween 5% non-fat dry milk at RT, the membranes were incubated overnight at 4ºC with the serum from patient CUN-28336. Patient serum was provided by the Biobank of the University of Navarra and were processed following standard operating procedures approved by the Ethical and Scientific Committee (2019.217 CEI-CUN). After extensive wash with TBS-Tween, the membranes were incubated with a horseradish peroxidase (HRP)-conjugated secondary antibody at RT for 1h. The substrate of the enzyme was provided by the reagents of SuperSignalTM West Dura Extended Duration Substrate (Thermo Scientific) and the signal was detected by the ODYSSEY CLx near-infrared fluorescence imaging system.

RNA extraction and RT-qPCR

Total RNA from liver samples was isolated using TRI Reagent® (Sigma,) according to the manufacturer's instructions. Total RNA was pre-treated with DNAse I using the TURBO DNAfree ™ Kit (Applied Biosystems) and retro-transcribed into complementary DNA (cDNA) using M-MLV reverse-transcriptase (Invitrogen). Real-time quantitative polymerase chain reactions (RT-qPCR) were performed using iQ SYBR Green Supermix (BioRad) in a CFX96 Real-Time Detection System (BioRad) and primers as specified in supplementary materials. HDV strand-specificity was analyzed as described elsewhere [21]. GAPDH was used as a control housekeeping gene.

Immunofluorescence

Cells were fixed in PBS 4% PFA for 20 min at RT and permeabilized with PBS 0.1% Triton X-100 for 15 min at RT prior incubation with PBS-0.1% tween 5% BSA (blocking buffer) for 30 min at 37ºC. After washing, cells were incubated for 30 min at 37ºC with with the serum from patient CUN-28336 at dilution 1:2500. Then, cells were incubated with the secondary antibody (goat anti-human IgG conjugated to Alexa Fluor 488, Life Technologies) at dilution 1:3000 for 30 min at 37ºC, protected from light. Finally, samples were covered with mounting medium containing DAPI (1.5µg/ml, Vector Laboratories), and the fluorescent samples were visualized with a confocal microscope (Zeiss LSM 880).

 doi:10.20944/preprints202103.0411.v1

Infectivity studies

Huh7-hNTCP cells were seeded in 12-well plates with coverslips, and maintained in DMEM 10% FBS 2% DMSO. The day of infection, colture medium was replaced by 1mL of supernatant collected from Huh-7 cotransfected with HBV/HDV WT or HBV/HDV-mutants at 7 and 14 dpt. The day after infection, the medium was replaced by fresh DMEM 2% FBS 2% DMSO, and at 7 dpi cells were fixed in 4% PFA, and the presence of HDAg-positive cells was examined by performing immunofluorescence, as indicated above.

Statistical Analysis

Statistical analyses were performed using GraphPad Prism 8.0 software. The data are presented as individual values ± standard deviation. Statistical significance was determined using unpaired t-test for single comparisons and two-way ANOVA followed by Bonferroni's multiple comparison tests to find differences between groups. *$p < 0.05$, ** $p < 0.01$, *** $p < 0.001$, **** $p < 0.0001$.

3. Results

3.1 Selection of the human hepatic cell line for the in vitro analysis of HDV mutants

HepG2 and Huh7 cells were transfected with equal amounts of a plasmid carrying 1.2x copies of the replication-competent HDV WT genome under the transcriptional control of a liver specific promoter previously described [21]. Cells were collected 1, 3, 7, 10, and 14 days post-transfection and were only split at day 7 (Figure 1A). The presence of HDV genomes and antigenomes and the induction of IFN-β and MxA expression were analysed by qRT-PCR, and HDAgs expression was analysed by Western blot.

Not surprisingly, HDV antigenomes were detected 24 hours after plasmid transfection in both cell lines, since the antigenome is the transcriptional product of the shuttle plasmid, then the levels increased up to day 7 in HepG2 cells decreasing thereafter, while in Huh7 cells HDV antigenome copies continued increasing up to day 14 (Figure 1B). HDV genomes were detected in both cell lines, indicating that HDV replication is initiated after plasmid transfection. In HepG2 cells, HDV genomes were detected at day 7 and, as observed for the antigenome, decreased thereafter. In Huh-7 cells, HDV genomes were detected 1 dpt and the levels increased for the entire duration of the experiment. In both cell lines, the shuttle plasmid was lost with time indicating that HDV replication is self-sustained and not entirely dependent on the presence of the transfected plasmid (Figure A1). Regarding HDAgs expression, S-HDAg was detected in both cell lines at day 3 (Figure 1C). In HepG2 S-HDAg is the only isoform detected, and its expression decreased at day 14 (Figure 1C). In Huh-7 cells S-HDAg expression increased with time and L-HDAg was detected 10 dpt increasing 14 dpt (Figure 1C). Thus, while Huh7 cells support a continue replication and antigen expression of HDV, viral replication in HepG2 cells decreases over time and gene editing either does not occur at all or it does at a very low frequency, since no L-HDAg was detected.

In order to understand the different behaviour of these two types of human hepatic cell lines, and since it has been recently reported that type I IFN strongly suppresses cell division-mediated spread of HDV genomes [27], we analysed IFN-β and MxA expression in both cell lines after HDV-plasmid transfection. While in Huh-7 cells IFN-β mRNA was barely detected, in HepG2 cells IFN-β and MxA were highly expressed at 10 dpt, 3 days after the cells were splitted (Figure 1D). These results indicate that most likely the differences found between HepG2 and Huh-7 cells were due to the HDV-sensing by the innate immune system and the induction of type I IFN response that blocks the spread of HDV in dividing HepG2 cells. Thus, Huh7 cell line was selected as the cellular platform for the characterization of HDV mutants.

3.2 In vitro analysis of HDV mutants

Three different HDV mutants were generated: HDV defective in the expression of both antigens (HDV-ΔHDAg), HDV defective in the expression of S-HDAg (HDV-ΔS-HDAg) and HDV defective in the expression of L-HDAg (HDV-ΔL-HDAg).

Preprints (www.preprints.org) | NOT PEER-REVIEWED | Posted: 16 March 2021 doi:10.20944/preprints202103.0411.v1

The experiment was performed as described in Figure 1A. As expected, no HDAg expression was detected in HDV-ΔHDAg transfected cells (Figure 2A) and the HDV antigenome sequence was detected at very low levels. In cells transfected with HDV-ΔS-HDAg, L-HDAg was transiently expressed at day 3 and only the HDV antigenome sequence was detected and dissapeared with time (Figure 2B). Transfection with the HDV-ΔL-HDAg mutant resulted in the expression of S-HDAg from 7 dpt that increased with time and both HDV genome and antigenome were detected at similar levels to those found in cells transfected with HDV WT. The analysis of HDAg expression by IF in HDV WT and HDV-ΔL-HDAg transfected cells showed a preferential localization of HDAgs in the nuclear compartment at 7 and at 14 dpt, but, while in HDV WT transfected cells the HDAgs were detected both in the nucleus and in the cytoplasm at 14 dpt, in cells transfected with the HDV-ΔL-HDAg mutant the HDAgs remained mainly in the nucleus (Figure 2C). Cell fractionation studies corroborated this observation showin a clear retection of the HDAg in the nuclear fraction (Figure 2D).

Then, we tested whether HDV infectious particles could be produced in the absence of L-HDAg. For that purpose, Huh7 cells were cotransfected with HBV plasmid and either HDV WT or HDV-ΔL-HDAg, supernatants were harvested at 7 and 14 dpt and added to Huh7 cells expressing the HBV/HDV receptor (hNTCP). As shown in Figure 2E, Huh7 cells cotransfected with the HDV WT plasmid are able to produce HDV infectious particles that were more abundant at 14 dpt than at 7 dpt; on the contrary, no HDV infective particles were produced in cells tranfected with mutant lacking L-HDAg.

3.3 In vivo virological analysis of HDV mutants

For the *in vivo* analysis, hepatotropic AAV vectors (serotype 8) were generated to convey the HDV genomes to the liver of mice. AAV-HDV WT, AAV-HDV-ΔHDAg, AAV-HDV-ΔL-HDAg, AAV-HDV-ΔS-HDAg were co-injected together with AAV-HBV. Animals were sacrificed 21 days after AAV injection for liver collection and HDV replication and HDAg expression were analysed. No HDAg expression or HDV genomes were detected in the liver of mice that received HDV-ΔS-HDAg or HDV-ΔHDAg (Figure 3A,B). The levels of HDV genome and antigenome in the in HDV-ΔL-HDAg injected mice were similar to those obtained in the HDV WT group (Figure 3A). Moreover, only the S-HDAg was detected by WB, and at levels significantly higher than in the animals injected with AAV-HDV WT (Figure 3B,C). Furthermore, immunohistochemistry analysis of HDAg expression in liver sections revealed a slightly higher percentage of HDAg positive cells in HDV-ΔL-HDAg than in HDV WT (Figure 3) that cannot be attributed to the presence of more AAV genomes (Figure A2A).

3.4 Effect of HDV mutants on Liver Damage

After AAV intravenous administration, animals were weekly bled to biochemically analyze the presence of liver damage, and they were sacrificed twenty-one days post-infection (dpi) to evaluate liver histology. The results revealed that the administration of HDV-ΔL-HDAg induced a significanly higher transaminase elevation than that induced by HDV-WT (Figure 4A-B). Liver histology in both groups was characterized by the presence of inflammatory foci and hepatocyte hypertrophy and necrosis that were more pronounced in the HDV-ΔL-HDAg group. Most of the hepatocytes showed pyknotic and enlarged nuclei (Figure 4B). The HDV-ΔL-HDAg group showed a significant increase in both the hepatocyte nuclear size (Figure 4C) and the number of hepatocytes undergoing apoptosis (activated caspase 3 positive cells) (Figure 4D) in comparison to the HDV WT group.

3.5 Analysis of liver inflammatory infiltrate and cytokine expression

For a better characterization of the HDV-ΔL-HDAg mutant, animals were treated as previously described and sacrificed 7, 14 and 21 dpi and livers were extracted.

The presence of macrophages (F4/80+ cells) and both CD8+ and CD4+ T cells was detected by immunostaining of liver sections and quantified. The analysis revealed higher amounts of immune cells in mice injected with the HDV-ΔL-HDAg mutant than in HDV-WT mice (Figure 5A).

Preprints (www.preprints.org) | NOT PEER-REVIEWED | Posted: 16 March 2021 doi:10.20944/preprints202103.0411.v1

Next we analysed the hepatic expression the following cytokines: IFN-β, IL-1β, IFN-γ, IL-6, TNF-α, and TGF-β. IFN-β was significantly higher in HDV-ΔL-HDAg than in HDV-WT at day 14 in association with the presence of more HDV genomes at the day 14 (Figure A2B), and no difference was found at day 21 (Figure 5B). Moreover, the expression of the pro-inflammatory cytokines IL-1β, IFN-γ, IL-6, TNF-α, and TGF-β was higher in HDV-ΔL-HDAg mice than in HDV-WT at days 14 and 21 post-infection, in agreement with the increased liver damage at these time points, however only the expression of TNF-α was significantly higher (Figure 5B).

3.6 Production of Infectious Viral particles

Since we have previously shown that immunocompetent C57BL/6 mice produced antibodies against HBV surface antigens able to block HDV infection [21], in this experiment B and T cell deficient RagB6 mice were used. Animals were injected as described before and serum obtained at day 21 were used to infect Huh7.5.1-hNTCP cells. As shown in Figure 6, while a significant number of HDAg-positive cells were detected in the cells infected with serum from HBV/HDV WT injected mice, no infective virions were detected in the serum obtained from HBV/HDV-ΔL-HDAg injected mice. Very, interestingly, when we analysed the severity of liver damage in these immunodeficient animals no differences in its magnitude were observed in comparison to WT animals. No significant differences were observed in serum transaminase values (Figure 7A), and liver histology (Figure 7B) and the number of activated caspase 3 positive cells (Figure 7C) was similar, indicating that the stronger liver damage observed in HDV-ΔL-HDAg is not associated to a T cell mediated response (Figure 7).

3.7 Effect of L-HDAg expression over the hepatic damage induced by HDV-ΔL-HDAg

In order to clarify if the L-HDAg can modulate the damage induced by the HDV mutant expressing only the S-HDAg, animals were co-injected with equal amounts of HDV-ΔL-HDAg and HDV-ΔS-HDAg. In order to administered the same amount of AAV vector to all the animals the HDV-ΔHDAg vector was used as negative control vector. Thus, animals were divided in 5 groups (n=4). Group 1: AAV-HBV+AAV-HDV WT+HDV-ΔHDAg vector, group 2: AAV-HBV+HDV-ΔL-HDAg+HDV-ΔHDAg, group 3: AAV-HBV+HDV-ΔL-HDAg+HDV-ΔS-HDAg, group 4: AAV-HBV+HDV-ΔHDAg+HDV-ΔS-HDAg, group5: 3x HDV-ΔHDAg. Transaminase analysed weekly after vector injection revealed a significant reduction of liver damage in animals receiving HDV-ΔL-HDAg and HDV-ΔS-HDAg in comparison to animals receiving HDV-ΔL-HDAg alone (Figure 8A). Moreover, liver histology reflected the biochemical findings, with a nearly normal histology in the animals receiving both mutants in comparison to those receiving only HDV-ΔL-HDAg, indicating all together that an early expression of L-HDAg ameliorates AAV-HDV-ΔS-HDAg induced liver damage. Furthermore, the analysis of HDV replication revealed that L-HDAg has a significant impact on HDV replication levels (Figure 8C).

3.2. Figures

Preprints (www.preprints.org) | NOT PEER-REVIEWED | Posted: 16 March 2021 doi:10.20944/preprints202103.0411.v1

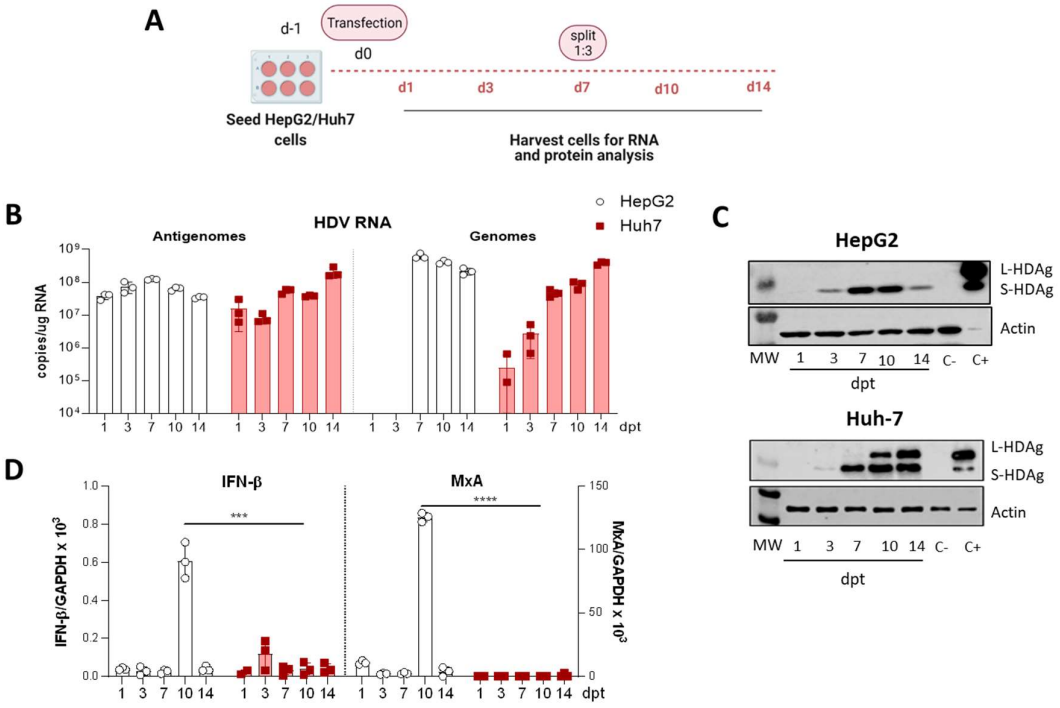

Figure 1. HDV life cycle is supported in Huh-7 cells upon transfecting HDV-encoding plasmid but not in HepG2 cells due to the activation of IFN-β signalling pathway. **(A)** Schematic representation of the experimental layout. HepG2 or Huh-7 cells were seeded and transfected with equal amounts of the plasmid encoding the HDV antigenome. For RNA and protein analysis, cells were collected at 1, 3, 7, 10 and 14 days post-transfection (dpt), and cells were split 1:3 at day 7. **(B)** Total RNA was extracted from cells and HDV antigenome and genome levels were assessed by RT-qPCR. **(C)** Western Blot analysis of HepG2 and Huh-7 cell lysates was performed to detect S-HDAg and L-HDAg. Positive control (C+): Huh-7 cells transfected with plasmids expressing S-HDAg and L-HDAg antigens and collected at 3 dpt. Negative control (C-): untransfected Huh-7 cells. **(D)** IFN-β (left) and MxA (right) expression levels were quantified by RT-qPCR and normalized using GAPDH as housekeeping gene. Statistical analysis using Mann Whitney test revealed differences between the two cell lines (***P<0.001, ****P<0.0001).

Preprints (www.preprints.org) | NOT PEER-REVIEWED | Posted: 16 March 2021 doi:10.20944/preprints202103.0411.v1

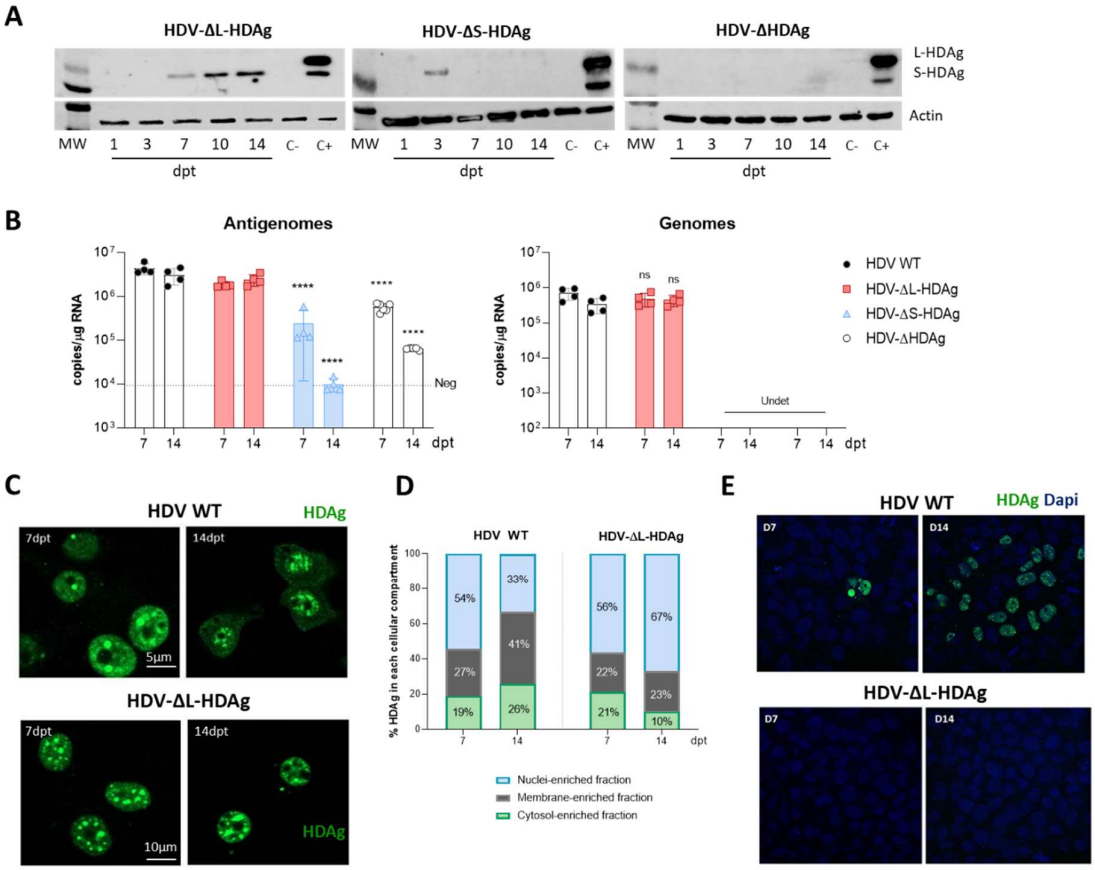

Figure 2. HDV mutants affecting S-HDAg and L-HDAg expression were generated and characterized in Huh-7 cells. (A) HDAg expression was assessed in Huh-7 cell lysates by Western Blot at 1, 3, 7, 10 and 14 dpt. **(B)** HDV genomes were produced after transfection with the plasmids that support S-HDAg expression: HDV WT and HDV-ΔL-HDAg). **(C,D)** HDAg localization was examined by immunofluorescence and by cell fractionation. The percentage of HDAgs present in the cytosolic-, the membrane- and the nuclear-enriched fractions was determined at 7 and 14 dpt. **(E)** Huh-7.5.1-hNTCP cells were infected with supernatants from HBV/HDV WT and HBV/HDV-ΔL-HDAg co-transfected cells collected at days 7 and 14 post-transfection. At 7 days post-infection (dpi), cells were fixed and immunostained with human serum for HDAg detection.

Preprints (www.preprints.org) | NOT PEER-REVIEWED | Posted: 16 March 2021 doi:10.20944/preprints202103.0411.v1

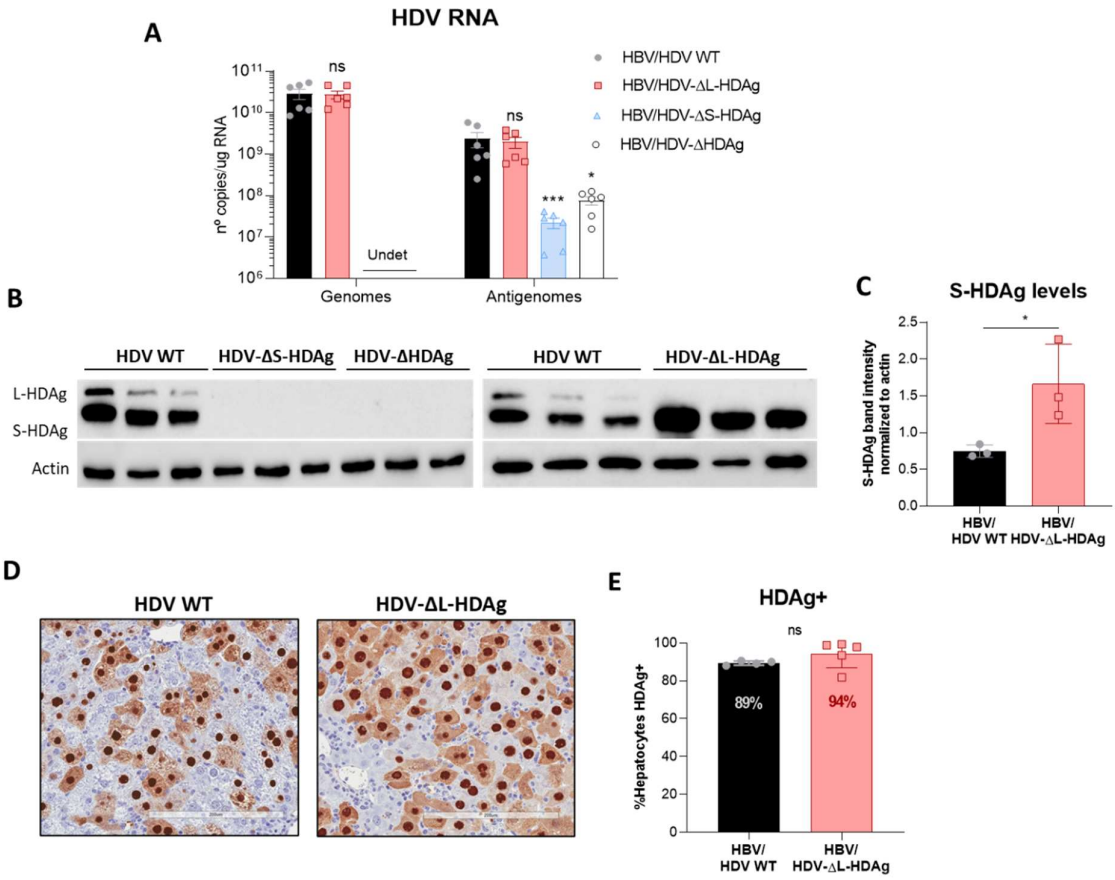

Figure 3. Administration of AAV-HDV mutants lacking the expression of S-HDAg resulted in a loss of HDV replication, while the absence of L-HDAg enhances S-HDAg production. Eight-week-old C57BL/6 WT mice received (n = 6) 5 ×10^{10} genome copies of AAV-HDV, AAV-HDV-ΔL-HDAg, AAV-HDV-ΔS-HDAg and AAV-HDV-ΔHDAg in combination with 5 ×10^{10} genome copies of AAV-HBV. **(A)** HDV genomes and antigenomes were analysed in livers of infected mice at 21 dpi (significant differences were determined by Kruskal-Wallis test and Dunn's post-test). **(B)** Western blot analysis of liver samples revealed the absence of HDAgs in mice receiving AAV-HDV-ΔS-HDAg and AAV-HDV-ΔHDAg and only the S-HDAg was detected in livers of mice receiving the HDV-ΔL-HDAg vector. **(C)** The levels of S-HDAg were compared between the HDV WT and HDV-ΔL-HDAg groups by densitometry. **(D)** Immunostaining against HDAgs was performed at 21 dpi in liver sections of mice injected with the AAV-HDV WT and AAV-HDV-ΔL-HDAg vectors. Scale bar: 200 μm. **(E)** HDAgs-positive cells were quantified in both groups of mice (n = 4). Mann-Whitney test revealed significant differences in S-HDAg protein levels and no differences between the percentage of HDAg-positive cells at 21 dpi (*P<0.05).

Preprints (www.preprints.org) | NOT PEER-REVIEWED | Posted: 16 March 2021 doi:10.20944/preprints202103.0411.v1

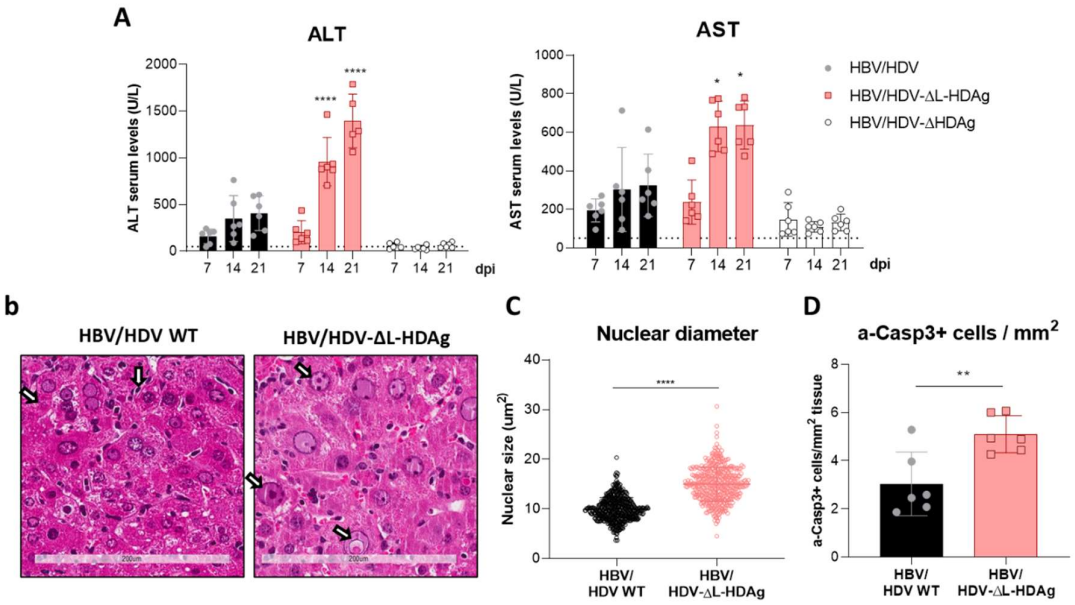

Figure 4. **The expression of the S-HDAg in the absence of L-HDAg resulted in an increased liver damage. (A)** Peripheral blood was collected every 7 days after vector injection to measure ALT and AST concentration in serum. Individual data points and mean values ±standard deviation are plotted; significant differences between groups at each time point are determined by two-way ANOVA followed by Bonferroni's multiple-comparison test. **(B)** Liver sections from AAV-HBV/HDV WT and AAV-HBV/HDV-ΔL-HDAg injected mice obtained 21 dpi were analyzed by H&E staining. Degenerated nuclei (white arrow) were observed in both group of mice but were more abundant upon infection with the HDV-ΔL-HDAg mutant. Scale bar: 200 μm. **(C)** The nuclear diameter was significantly bigger when only the S-HDAg was overexpressed. Significant differences were found by performing an unpaired t-test. **(D)** Immunostaining against cleaved caspase 3 revealed that S-HDAg overexpression exacerbates hepatocyte death by apoptosis. Statistical analysis using Mann Whitney test revealed differences between the two groups (*P<0.05, **P<0.01, ****P<0.0001).

Preprints (www.preprints.org) | NOT PEER-REVIEWED | Posted: 16 March 2021 doi:10.20944/preprints202103.0411.v1

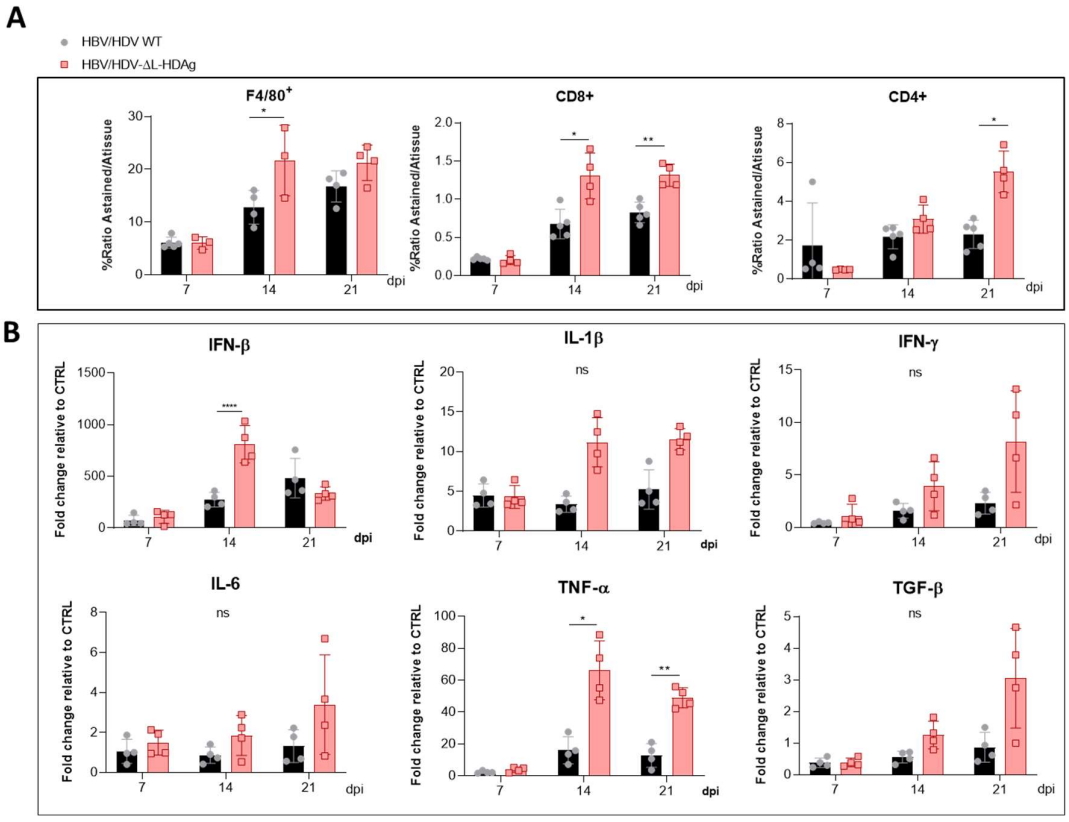

Figure 5. The HDV mutant expressing only the S-HDAg increased the recruitment of inflammatory cells and the release of pro-inflammatory cytokines. Liver sections collected at 7, 14 and 21 dpi of AAV-HBV/HDV WT and AAV-HBV/HDV-ΔL-HDAg injected mice were subjected to (**A**) F4/80-, CD4- and CD8 immunostaining to quantify the percentage of intrahepatic macrophages, CD4+ and CD8+ T lymphocytes, respectively, and **(B)** The expression levels of IFN-β, IFN-γ, IL-1β, IL-6, TNF-α and TGF-β were analysed by RT-qPCR. Significant differences between groups at each time point were determined by two-way ANOVA followed by Bonferroni's multiple-comparison test. *P<0.05, **<0.01, ****P<0.0001.

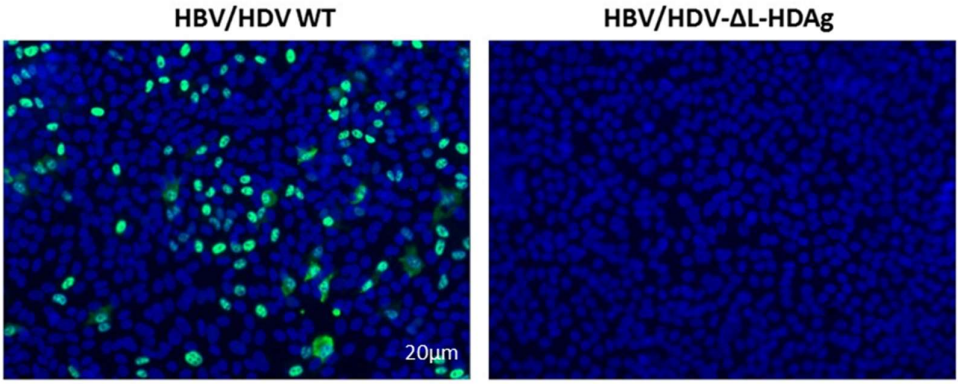

Figure 6. Infection of RagB6 mice with AAV-HBV/HDV-ΔL-HDAg failed to produce HDV infectious particles. Huh7-hNTCP cells were incubated with serum collected from AAV-HBV/HDV WT- and AAV-HBV/HDV-ΔL-HDAg infected RagB6 mice at 21 dpi. At 7 dpi, cells were fixed and immunostained to detect intracellular HDAg.

Preprints (www.preprints.org) | NOT PEER-REVIEWED | Posted: 16 March 2021 doi:10.20944/preprints202103.0411.v1

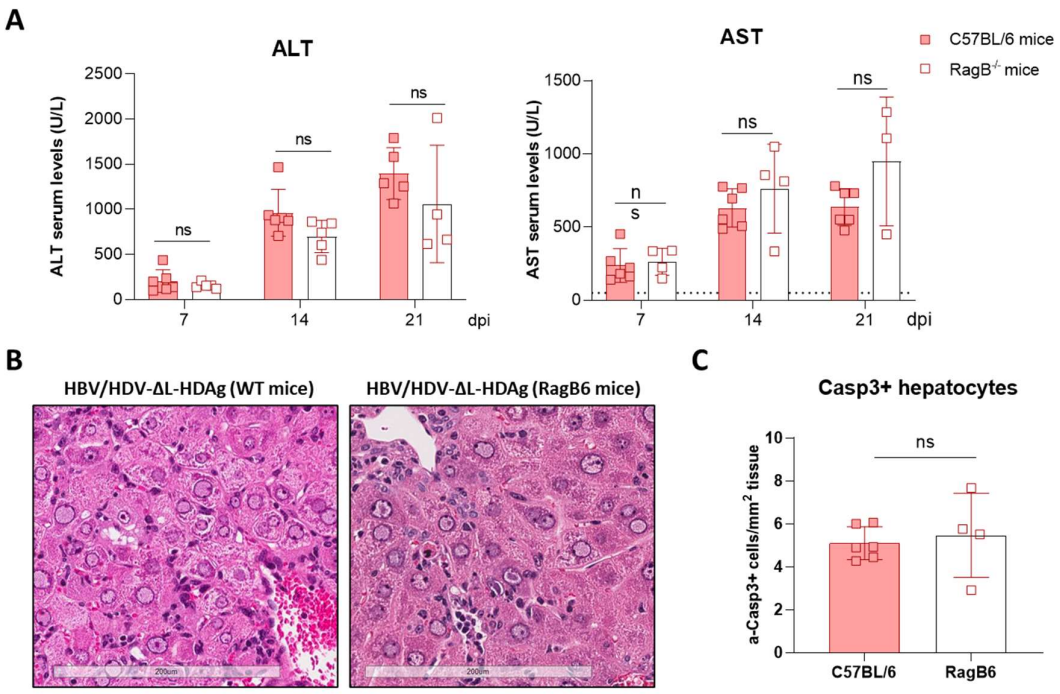

Figure 7. The liver damage triggered by the HDV mutant expressing only S-HDAg is independent of B- and T lymphocytes and Natural Killer T (NKT) cells. Eight-week-old WT (n = 4) and RagB6 mice (n = 4) received 5×10^{10} genome copies of AAV-HDV-ΔL-HDAg and AAV-HBV. **(A)** Transaminase levels were analysed at 7, 14 and 21 dpi. Individual data points and mean values ± standard deviation are plotted; no significant differences were observed between WT and RagB6 mice injected with AAV-HBV/HDV-ΔL-HDAg by performing two-way ANOVA and Bonferroni multiple-comparison test**. (B)** Examination of liver sections by H&E showed no histological differences between WT and RagB6 mice at 21 dpi. Scale bar: 200 μm. **(C)** Liver sections of WT and RagB6 mice receiving AAV-HDV-ΔL-HDAg sacrificed at 21 dpi were analyzed by IHC for activated Caspase 3. Mann Whitney test did not reveal significant differences.

Preprints (www.preprints.org) | NOT PEER-REVIEWED | Posted: 16 March 2021 doi:10.20944/preprints202103.0411.v1

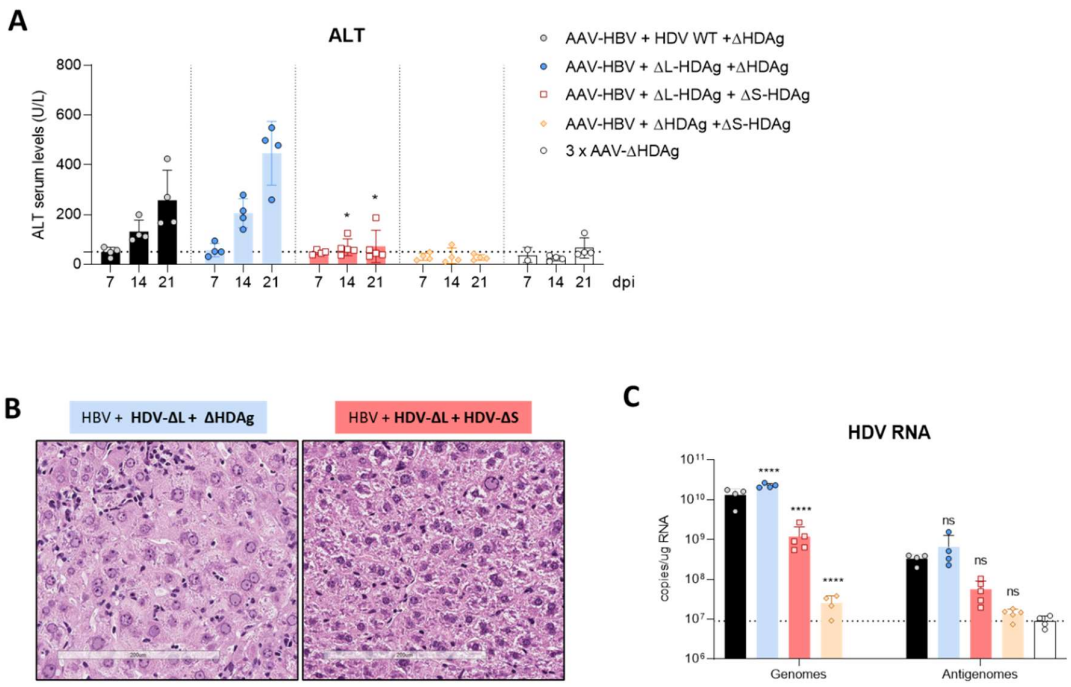

Figure 8. Expression of L-HDAg at the beginning of HDV life cycle decreased liver damage and HDV replication. (A) Peripheral blood was collected weekly after the administration the different combination of AAV vectors and ALT concentration in serum was measured. Individual data points and mean values ± standard deviation are plotted; significant differences between HBV/ΔL-HDAg/ΔHDAg and HBV/ΔL-HDAg/ΔS-HDAg groups at each time point were determined by two-way ANOVA followed by Bonferroni multiple-comparison test. The dotted line represents the ALT ULN, 50 U/L. **(B)** Histological analysis of liver sections by H&E showed visible alteration in the HBV/ΔL-HDAg/ΔHDAg that were not present in the HBV/ΔL-HDAg/ΔS-HDAg group. Scale bar: 200 μm. **(C)** Total RNA was extracted from infected livers to quantify HDV genome and antigenome levels at 21 dpi by RT-qPCR. Significant differences between HBV/HDV WT/ΔHDAg and the rest of the groups groups were determined by two-way ANOVA followed by Bonferroni multiple-comparison test. The dotted line represents background. *P<0.05, ****P<0.0001.

4. Discussion

HDV infection is responsible for the most severe form of viral hepatitis in humans, leading to cirrhosis in 80% of cases within 10 years, and with a significant proportion of patients dying of hepatic decompensation [1,3]. The mechanism involved in the severity of the disease remains obscure largely because of the lack of appropriated small animal models in which *in vivo* molecular analysis can be performed. Recently, we have developed a HDV mouse model that overcome species related limitations based on the transfer to mouse hepatocytes of the HDV replication competent genome via an AAV vector, as previously described for HBV [21]. For the first time, HDV-mediated liver injury was observed in mice, in association with a strong inflammatory infiltrate and hepatocyte apoptosis. Furthermore, we found that TNF-α was partially responsible for the observed liver damage. The beauty of this model is that animals with different genetic background can be used, and that mutation in the HDV genome can be easily introduced and tested in mice [21, 26].

Pioneering work performed in the 80-90's by a number of prominent virologist demonstrated the role of HDAgs in the viral cycle and in the induction of cell damage [12,13,18,19,28,29]. Those studies were performed using different cellular systems and transfection of HDV-shuttle plasmids. Here, using

Preprints (www.preprints.org) | NOT PEER-REVIEWED | Posted: 16 March 2021 doi:10.20944/preprints202103.0411.v1

AAV vector as HDV delivery platform, we have tested *in vivo* the role of of HDAg in the the viral life cycle and in the induction of liver damage.

We have generated three different mutants with altered expression of HDAgs: one lacking HDAg expression, the second one expressing only the L-HDAg, and the third one expressing only the S-HDAg. The initial characterisation of the mutants was performed by *in vitro* plasmid transfection. Firstly, HepG2 and Huh7 cells were transfected with plasmids carrying the HDV WT sequence. While in Huh7 cells HDV replication and HDAg expression were sustained despite cell passages and loss of the shuttle plasmid, in HepG2 both, replication and antigen expression, decreased after splitting the cells. Furthermore, both HDV antigens were expressed in Huh7 cells but only the S-HDAg was detected in HepG2. The different behaviour of these two cell lines can be explained by differences in the activation of the innate immune response. A strong type I IFN response was detected in HepG2 cells but not in Huh7 cell, suggesting that after cell division and disruption of the nuclear membrane the HDV RNA genomes present in the nucleus are sensed by MDA5, initiating the activation of the innate immune response in HepG2 but not in Huh7 cells. Very recently Zang et al., have indicated that HDV "self-induced" IFN response restricts HDV amplification in HepaRG cells [25] and this would explain why HDV replication is sustained in Huh7 but not in HepG2 cells. Thus Huh7 cells were selected for the characterization of the HDV mutants.

Both *in vitro* and *in vivo* studies showed that the HDV genome itself is unable to initiate replication and requires the expression of the viral antigens, indicating that the interaction between the cellular polymerase and the viral genome requires the intervention of the HDAg that cannot be replaced by a host protein. More interestingly, the S-HDAg cannot be replaced by the large antigen despite both sequences being identical except for the 19 extra aminoacid at the carboxy terminal region of the L-HDAg. On the other hand, we also found *in vitro* that the L-HDAg is essential for the export of the HDV RNP from the nucleus to the cytoplasm as well as for the formation of HDV infective particles, and cannot be substituted by the S-HDAg.

However, in mice the absence of L-HDAg did not preclude the presence of HDAg in the cytoplasm of the mice. Interestingly, both S-HDAg expression levels and HDV replication were significantly higher in the mutant lacking L-HDAg expression, pointing towards the regulatory role of the L-HDAg in the inhibition of HDV replication. Furthermore, while the production of the antigenome sequence alone or in the presence of L-HDAg had no effect on liver damage, the expression of S-HDAg alone resulted in a significant increase in liver damage in comparison to the one induced by the injection of the AAV carrying the HDV WT genome. We observed a significant enlargement of hepatocyte nuclei and the presence of a considerable number of aberrant hepatocytes with a higher frequency og apoptotic cells. We also found that the liver of these animals showed a more prominent inflammatory infiltrate in comparison to HDV WT injected mice (with significant higher numbers of macrophages and T cells), resulting in a higher expression levels of TNFα which we previously showed to play a significant role in HDV-induced liver damage [26]. Interestingly, the experiment performed in RagB6 mice to demonstrate the essential role of the L-HDAg in the formation of HDV infectious particles, also showed that T cells are not directly involved in the exhacerbation of the liver disease induced by the mutant expressing only the S-HDAg, indicating a potential major role of a direct cytoxic effect of the small antigen. Our results are in line with previous data generated the 90's demonstrating a direct cytotoxicity of the S-HDAg but not of the L-HDAg [11-13]. It was also observed that cells stably transfected with a replication competent HDV construct showed spontaneous death that diminished when the expression of L-HDAg was detected [13]. Furthermore, it was reported that the ratio L-HDAg/S-HDAg is higher in patients with chronic HDV infection and low transaminase levels than in patients with HDV acute infection and high transaminase levels [30,31], suggesting, as we observed here, a major role of the S-HDAg in the development of HDV-induced liver damage that is attenuated by L-HDAg expression.

In fact, we found that the coadministration of the mutant expressing only the L-HDAg and the mutant expressing only the S-HDAg, which resulted in an early expression of both antigens, significantly ameliorated the liver damage induced by the mutant that only expresses the S-HDAg. L-HDAg modulates the activity of S-HDAg and reduces both HDV replication and S-HDAg expression levels.

This is a very interesting finding considering that in patients both non-edited and edited forms of the HDV genomes can be found in the circulation [32, 33], indicating that at infection patients receive two types of viral particles: one, the non-edited form, expressing S-HDAg very early and initiating viral replication, and the other, the edited genome, expressing only L-HDAg and unable to inititate replication. We hypotesise that the latter form can play an important role in regulating the initial levels of S-HDAg expression and viral replication, as well as the concomitant induction of the innate immune antiviral response and cell cytotoxicity. Using this strategy, the virus would avoid the death of the infected cells and the clearance by the immune system, with an advantage for the survival of the virus as well as the host cell. These findings are consistent with the hypothesis that the L-HDAg may promote viral persistence by ameliorating liver damage.

In summary, the use AAV-HDV/AAV-HBV has allowed us us to confirm in vivo the properties attributed to the HDV-antigens in the HDV life cycle previously describe in cell culture. But more importantly, we showed the major role of HDAg in the HDV-induced liver pathology that was described in vitro in the early 90', and that we showed is T cell independent. Thus, AAV mediated delivery of hepatitis virus replication competent geneomes represents a very attractive platform to determine the mechanism of HDV-induced liver pathology and for the development of new and more efficient treatments.

Author Contributions: Conceptualization, R.A. and G.G.A.; methodology, A.V. and C.O.; formal analysis.S.M., N.G.E. and G.C.; investigation, S.M., N.G.E., G.C., C.U. and L.S.A..; ; writing—original draft preparation, S.M and N.G.E.; writing—review and editing, C.U., R.A. and G.G.A.; supervision, R.A. and G.G.A..; funding acquisition, G.G.A. All authors have read and agreed to the published version of the manuscript

Funding This research was funded by RTI2018-101936-B-I00 to G.G-A. from Secretaria de Estado de Investigación, Desarrollo e Innovación, Ministerio de Economia y Competitividad and Ministerio de Ciencia y tecnología. Lester Suarez was supported by an FPU fellowship from the Spanish Ministry of Education, Carla Usai and Gracian Camps were supported by FPI fellowships from the Spanish Ministry of Economy and Competitiveness and Sheila Maestro was supported by FIMA's fellowship.

Acknowledgments: We particularly acknowledge the patients for their participation and the Biobank of the University of Navarra for its collaboration. We thank Professor John Taylor, Professor Frank Chisari and Dr Urtzi Garaigorta for providing us with essential reagents for our study. We are grateful to Elena Ciordia, Alberto Espinal, and CIFA staff for animal care and vivarium management and to Laura Guembe for technical assistance.

Conflicts of Interest: "The authors declare no conflict of interest in relation with the work presented in this manuscript."

Appendix

Preprints (www.preprints.org) | NOT PEER-REVIEWED | Posted: 16 March 2021 doi:10.20944/preprints202103.0411.v1

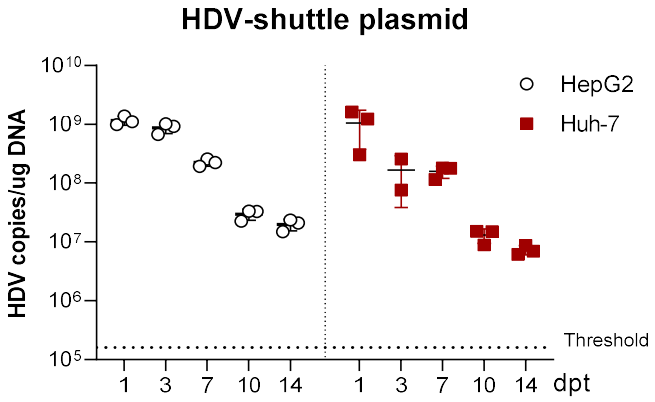

Figure A1. The levels of shuttle plasmid containing the HDV antigenome decrease over time associated to cell division. Total DNA was extracted from HepG2 and Huh7 cells and HDV DNA copies were quantified by qPCR.

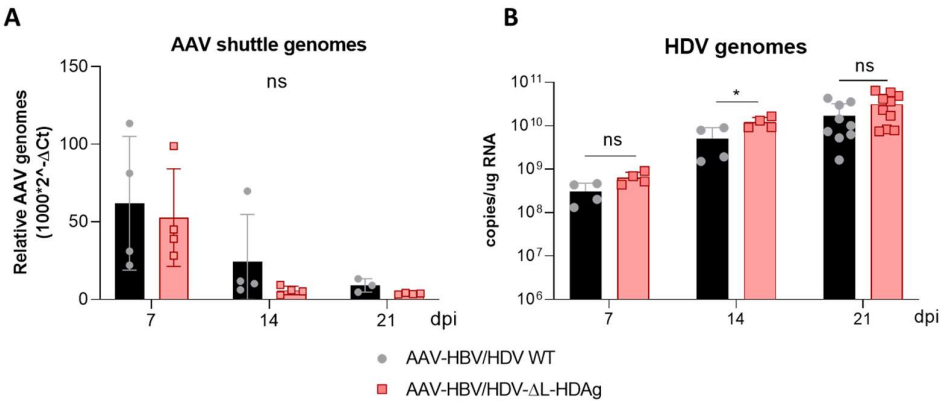

Figure A2. HDV genome copies increase with time in C57BL/6 mice after AAV-HDV WT or AAV-HDV-ΔL-HDAg ijection while the AAV genomes drop during the experiment. **(A)** HDV RNA was analysed in livers of mice injected with AAV-HDV WT and AAV-HDV-ΔL-HDAg by RT-qPCR. **(B)** Total DNA was extracted from infected livers and AAV-HDV genomes were quantified by qPCR. Statistical analysis by two-way ANOVA showed significant differences in HDV RNA at 14 dpi. *P<0.05.

References

1. Z. Miao, S. Zhang, X. Ou, S. Li, Z. Ma, W. Wang, et al. Estimating the global prevalence, disease progression and clinical outcome of hepatitis delta virus infection J Infect Dis, 221 (2020), pp. 1677-1687.
2. A.J. Stockdale, B. Kreuels, M.Y.R. Henrion, E. Giorgi, I. Kyomuhangi, C. de Martel, et al. The global prevalence of hepatitis D virus infection: systematic review and meta-analysis J Hepatol, 73 (2020), pp. 523-532.
3. Chen HY, Shen DT, Ji DZ, Han PC, Zhang WM, Ma JF, et al. Prevalence and burden of hepatitis D virus infection in the global population: a systematic review and meta-analysis. Gut 2019; 68: 512- 521.
4. Kamal H, Westman G, Falconer K, Duberg AS, Weiland O, Haverinen S, Wejstål R, Carlsson T, Kampmann C, Larsson SB, Björkman P, Nystedt A, Cardell K, Svensson S, Stenmark S, Wedemeyer H, Aleman S. Long-Term Study of Hepatitis Delta Virus Infection at Secondary Care Centers: The Impact of Viremia on Liver-Related Outcomes. Hepatology. 2020 Oct;72(4):1177-1190.

5. Palom A, Rodríguez-Tajes S, Navascués CA, García-Samaniego J, Riveiro-Barciela M, Lens S, Rodríguez M, Esteban R, Buti M. Long-term clinical outcomes in patients with chronic hepatitis delta: the role of persistent viraemia. Aliment Pharmacol Ther. 2020 Jan;51(1):158-166.
6. Koh C, Heller T, Glenn JS. Pathogenesis of and New Therapies for Hepatitis D. Gastroenterology. 2019 Jan;156(2):461-476.e1. doi: 10.1053/j.gastro.2018.09.058.
7. Deterding K, Wedemeyer H. Beyond Pegylated Interferon-Alpha: New Treatments for Hepatitis Delta. AIDS Rev. 2019;21(3):126-134. doi:10.24875/AIDSRev.19000080.
8. Shah PA, Choudhry S, Reyes KJC, Lau DTY. An update on the management of chronic hepatitis D. Gastroenterol Rep (Oxf). 2019 Oct 19;7(6):396-402.
9. Buitrago B, Popper H, Hadler SC, Thung SN, Gerber MA, Purcell RH, Maynard JE. Specific histologic features of Santa Marta hepatitis: a severe form of hepatitis delta-virus infection in northern South America. Hepatology. 1986 Nov-Dec;6(6):1285-91. doi: 10.1002/hep.1840060610.
10. Chu CM, Liaw YF. Studies on the composition of the mononuclear cell infiltrates in liver from patients with chronic active delta hepatitis. Hepatology. 1989 Dec;10(6):911-5. doi: 10.1002/hep.1840100603.
11. Lefkowitch JH, Goldstein H, Yatto R, Gerber MA. Cytopathic liver injury in acute delta virus hepatitis. Gastroenterology. 1987 May;92(5 Pt 1):1262-6. doi: 10.1016/s0016-5085(87)91086-9.
12. Cole SM, Gowans EJ, Macnaughton TB, Hall PD, Burrell CJ. Direct evidence for cytotoxicity associated with expression of hepatitis delta virus antigen. Hepatology. 1991 May;13(5):845-51.
13. Macnaughton TB, Gowans EJ, Jilbert AR, Burrell CJ. Hepatitis delta virus RNA, protein synthesis and associated cytotoxicity in a stably transfected cell line. Virology. 1990 Aug;177(2):692-8. doi: 10.1016/0042-6822(90)90535-y.
14. Mentha N, Clément S, Negro F, Alfaiate D. A review on hepatitis D: From virology to new therapies. J Adv Res. 2019 Mar 29;17:3-15. doi:10.1016/j.jare.2019.03.009.
15. Yan, H.; Zhong, G.; Xu, G.; et al. Sodium taurocholate cotransporting polypeptide is a functional receptor for human hepatitis B and D virus. Elife. 2013;1:e00049.
16. Ni Y, Lempp FA, Mehrle S, Nkongolo S, Kaufman C, Fälth M, Stindt J, Königer C, Nassal M, Kubitz R, Sültmann H, Urban S. Hepatitis B and D viruses exploit sodium taurocholate co-transporting polypeptide for species-specific entry into hepatocytes. Gastroenterology. 2014 Apr;146(4):1070-83.
17. Aldabe R, Suárez-Amarán L, Usai C, González-Aseguinolaza G. Animal models of chronic hepatitis delta virus infection host-virus immunologic interactions. Pathogens. 2015 Feb 12;4(1):46-65. doi: 10.3390/pathogens4010046.
18. Kuo MY, Chao M, Taylor J. Initiation of replication of the human hepatitis delta virus genome from cloned DNA: role of delta antigen. J Virol. 1989 May;63(5):1945-50. doi: 10.1128/JVI.63.5.1945-1950.1989.
19. Chao M, Hsieh SY, Taylor J. Role of two forms of hepatitis delta virus antigen: evidence for a mechanism of self-limiting genome replication. J Virol.1990 Oct;64(10):5066-9. doi: 10.1128/JVI.64.10.5066-5069.1990.
20. Polson AG, Bass BL, Casey JL. RNA editing of hepatitis delta virus antigenome by dsRNA-adenosine deaminase. Nature. 1996 Apr 04;380(6573):454-6.
21. Suárez-Amarán L, Usai C, Di Scala M, Godoy C, Ni Y, Hommel M, Palomo L, Segura V, Olagüe C, Vales A, Ruiz-Ripa A, Buti M, Salido E, Prieto J, Urban S, Rodríguez-Frias F, Aldabe R, González-Aseguinolaza G. A new HDV mouse model identifies mitochondrial antiviral signaling protein (MAVS) as a key player in IFN-β induction. J Hepatol. 2017 Oct;67(4):669-679. doi: 10.1016/j.jhep.2017.05.010.
22. Giersch K, Allweiss L, Volz T, Helbig M, Bierwolf J, Lohse AW, Pollok JM, Petersen J, Dandri M, Lütgehetmann M. Hepatitis Delta co-infection in humanized mice leads to pronounced induction of innate immune responses in comparison to HBV mono-infection. J Hepatol. 2015 Aug;63(2):346-53. doi:10.1016/j.jhep.2015.03.011.
23. Alfaiate D, Lucifora J, Abeywickrama-Samarakoon N, Michelet M, Testoni B, Cortay JC, Sureau C, Zoulim F, Dény P, Durantel D. HDV RNA replication is associated with HBV repression and interferon-stimulated genes induction in super-infected hepatocytes. Antiviral Res. 2016 Dec;136:19-31. doi:10.1016/j.antiviral.2016.10.006.
24. He W, Ren B, Mao F, Jing Z, Li Y, Liu Y, Peng B, Yan H, Qi Y, Sun Y, Guo JT, Sui J, Wang F, Li W. Hepatitis D Virus Infection of Mice Expressing Human Sodium Taurocholate Co-transporting Polypeptide. PLoS Pathog. 2015 Apr 22;11(4):e1004840. doi: 10.1371/journal.ppat.1004840.
25. Zhang Z, Filzmayer C, Ni Y, Sültmann H, Mutz P, Hiet MS, Vondran FWR, Bartenschlager R, Urban S. Hepatitis D virus replication is sensed by MDA5 and induces IFN-β/λ responses in hepatocytes. J Hepatol. 2018 Jul;69(1):25-35. doi:10.1016/j.jhep.2018.02.021.

26. Usai C, Maestro S, Camps G, Olague C, Suárez-Amaran L, Vales A, Aragon T, Hommel M, Aldabe R, Gonzalez-Aseguinolaza G. TNF-alpha inhibition ameliorates HDV-induced liver damage in a mouse model of acute severe infection. JHEP Rep. 2020 Mar 10;2(3):100098. doi: 10.1016/j.jhepr.2020.100098.
27. Zhang Z, Ni Y, Urban S. Endogenous and exogenous IFN responses suppress HDV persistence during proliferation of hepatocytes in vitro. J Hepatol 2019;70:e718-e719.
28. Bergmann KF, Cote PJ, Moriarty A, Gerin JL. Hepatitis delta antigen. Antigenic structure and humoral immune response. J Immunol. 1989 Dec 1;143(11):3714-21.
29. Denniston KJ, Hoyer BH, Smedile A, Wells FV, Nelson J, Gerin JL. Cloned fragment of the hepatitis delta virus RNA genome: sequence and diagnostic application. Science. 1986 May 16;232(4752):873-5. doi: 10.1126/science.3704630.
30. Bergmann KF, Gerin JL. Antigens of hepatitis delta virus in the liver and serum of humans and animals. J Infect Dis. 1986 Oct;154(4):702-6. doi: 10.1093/infdis/154.4.702.
31. Sureau C, Taylor J, Chao M, Eichberg JW, Lanford RE. Cloned hepatitis delta virus cDNA is infectious in the chimpanzee. J Virol. 1989 Oct;63(10):4292-7. doi: 10.1128/JVI.63.10.4292-4297.1989.
32. Sopena S, Godoy C, Tabernero D, Homs M, Gregori J, Riveiro-Barciela M, Ruiz A, Esteban R, Buti M, Rodríguez-Frías F. Quantitative characterization of hepatitis delta virus genome edition by next-generation sequencing. Virus Res. 2018 Jan 2;243:52-59. doi: 10.1016/j.virusres.2017.10.003.
33. Homs M, Rodriguez-Frias F, Gregori J, Ruiz A, Reimundo P, Casillas R, Tabernero D, Godoy C, Barakat S, Quer J, Riveiro-Barciela M, Roggendorf M, Esteban R, Buti M. Evidence of an Exponential Decay Pattern of the Hepatitis Delta Virus Evolution Rate and Fluctuations in Quasispecies Complexity in Long-Term Studies of Chronic Delta Infection. PLoS One. 2016 Jun 30;11(6):e0158557. doi: 10.1371/journal.pone.0158557.